Maximally Confined Silicon Microring and Microdisk Modulators and Switches

Michael R. Watts, Douglas C. Trotter, and Ralph W. Young

Applied Photonic Microsystems, Sandia National Labs, P.O. Box 5800, Albuquerque New Mexico 87185
mwatts@sandia.gov

Abstract

Silicon resonant microdisk and microring modulators and switches based on free-carrier depletion and injection were designed and fabricated with the aim of minimizing device radius to theoretical bend-radiation imposed limits. Minimizing device area serves to simultaneously maximize resonator free-spectral-range, minimize switching energy, and maximize component density, all critical parameters for wideband chip-to-chip and intrachip communication applications. Confinement of the bend-mode in the modulators is minimized by contacting the modulator from within the interior of the resonator to ensure a hard outer wall of the cavity. Both numerical and experimental results will be presented.

1. Introduction

As optical networks move from long-distance to short-reach applications, the need for high-speed, low-power, modulators and switches becomes increasing important. Recently, compact, high-speed, broadband Mach-Zehnder modulators and switches have been demonstrated in silicon [1,2]. However, many important applications, including supercomputers and intrachip networks, require fine-grain routing of data. Channel selective modulators and switches can provide the necessary granularity. Yet, to date, only first order modulators/switches have been constructed in silicon [3,4]. Such devices have Lorentzian band-passes that are unsuitable for the channel-selective switch application. Moreover, all such devices demonstrated to date require ridge waveguides limiting the modal confinement and resulting in small free-spectral-ranges (FSRs). These small FSRs limit the available communication line bandwidth.

Here, we present the results of the first high-speed silicon microphotonic channel-selective-switch. The switch demonstrates flat-top, 2nd-order ~40-GHz pass-bands. Using a new active microdisk design with a hard outer wall, we achieve disk radii of only R = 3µm enabling a 4.2THz FSR and a switching time of 2.4ns. Open eye-diagrams of 10Gb/s pseudo-random bit-streams are demonstrated in both states of the switch with ≥16dB on-off extinction. Further, we present results of reverse-biased modulators demonstrating a time constant of τ=120ps.

2. Discussion and Experimental Results

Finite-difference cylindrical modesolver simulations indicate that microring-resonators with bend radii as small as 2µm can be achieved so long as a hard outer wall of the microring is maintained (see Fig. 1a). Higher order filter responses (Fig. 1b) can then be generated by coupling multiple such microrings or microdisks together.
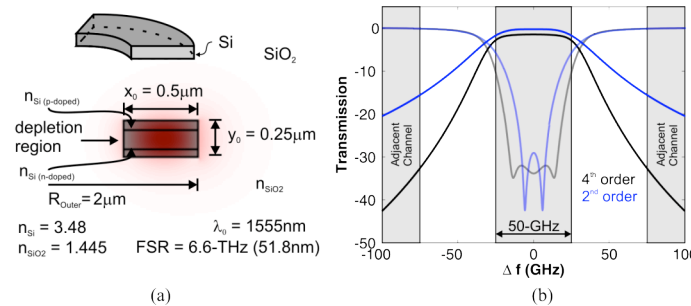
Figure 1. (a) Mode of an R = 2µm microring. The radiation or bend-loss limited Q is predicted by the modesolver to be $Q > 10^7$ in the undoped or fully depleted state. (b) Filter responses of 2nd order and 4th order filters constructed of R = 2µm microrings.

First- and second-order silicon microdisk modulators and switches with hard outer walls were designed and fabricated. A diagram and scanning electron micrograph (SEM) of a focused ion beam (FIB) cut through the center of the second-order silicon microdisk switch are presented in Fig. 2a and 2b, respectively. The switch consists of a pair of R=3µm radius microdisk resonators coupled together to provide a 2nd-order filter response. Smaller microdisk R=2µm structures were fabricated, but suffered from insufficient quality factors to be used in switch or modulator applications. The switch operates on the free-carrier-effect [5] in silicon and the vertical p-n junction used to inject and deplete carriers is depicted in Fig. 2c. By using a vertical junction and making contact from within the center of the disk, all contacts were kept within the interior of the microdisk enabling a hard outer silicon wall of the microdisk to be maintained. This is in contrast to all previously demonstrated silicon microring or microdisk modulators and it is this hard outer wall that enables maximum confinement of the whispering gallery mode with the realized 3µm bend radius. Further, the small resonator size enables the massive 4.2-THz demonstrated FSR (see Fig. 2d) critical for maximizing communication line bandwidth. While the switch can be operated at very high speeds (τ = 120ps) in a reverse-biased mode, wherein carriers are depleted, current doping levels are insufficient to provide the requisite >40GHz shift required to move the pass-band out of the way. To achieve such a large shift, carriers are injected into the structure by forward biasing the diode. Plots of the filter Thru and Drop port responses at λ_0 = 1501nm and λ_0 = 1533nm as a function of the drive current (and voltage) are provided in Fig. 2e and 2f, respectively. Both resonances demonstrate high-quality second-order filter responses with the corresponding second-order filter roll-off. The filter response shifts to higher frequencies with applied bias.
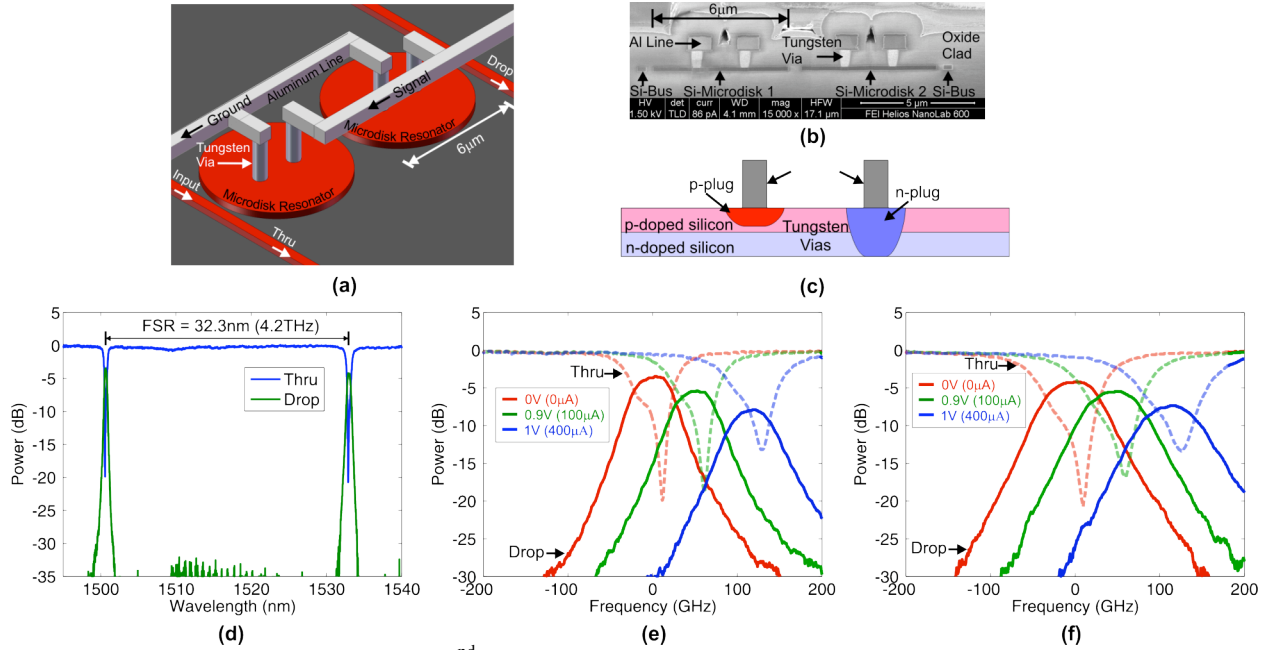

Figure 2. (a) Diagram of the fabricated 2nd order microdisk switch. (b) Scanning electron micrograph (SEM) image of a focused ion beam (FIB) cut through the center of the silicon microdisk switch. (c) Doping profile within microdisk switch. (d) Measured FSR of the 2nd order microdisk switch indicating FSR = 4.2-THz (32.5nm). (e) Measured spectral response of 2nd order microdisk switch as a function of applied voltage (λ_0 = 1501nm). The Drop port response has a 33-GHz 1-dB pass-band. (f) Measured spectral response of 2nd order microdisk switch as a function of applied voltage (λ_0 = 1533nm). The Drop port response has a 46-GHz 1-dB pass-band.

Frequency shifts of 50GHz and 117GHz are achieved with applied currents of 100µA and 400µA, respectively. At an applied current of 400µA, an extinction in the Drop port of >25dB is achieved at λ_0 = 1501nm and >20dB at λ_0 = 1533nm. Importantly, the filter shape at each resonance is maintained largely independent of the applied bias. The 1-dB passband at λ_0 = 1501nm is 33-GHz wide and the filter achieves peak extinction of 20dB in the Thru port. The 1-dB passband at λ_0 = 1533nm is 46-GHz wide and the filter achieves peak extinction of 20dB in the Thru port. Drop port losses for the λ_0 = 1501nm and λ_0 = 1533nm resonances are 3.5dB and 4dB, respectively. The Drop port loss is a result of several effects including bus-to-disk coupling loss, coupling to the substrate, and to a small extent free-carrier loss. A slight asymmetry exists in the filter Thru and Drop port responses as a result of a small

mismatch in the microdisk frequencies. This asymmetry was systematic (a positive slope from low-to-high frequency on all fabricated devices) and likely a result of mechanical or optical loading of the asymmetrically laid out metal contacts.

The switch was fabricated from a silicon-on-insulator (SOI) wafer with an initial 260nm silicon layer thickness and 1µm of buried oxide. The realized bus waveguide dimensions were 245nm×360nm, and the separations between the bus waveguides and the disk and between the disks were 285nm and 580nm, respectively, as measured by a scanning electron microscope (SEM). The switch geometry was defined with an ASML Deep Ultra-Violet (DUV) laser scanner and silicon reactive ion etch. Sacrificial oxidation was performed at 950°C to remove etch damage and a secondary high temperature (1100°C) oxidation step was performed to passivate the silicon sidewall in preparation for implantation. Subsequently, the diode implants for both the n and p portions of the junction were performed, followed by n+ and p+ plugs. Doping concentrations for the diode implants were $5 \cdot 10^{17} cm^{-3}$ and $10^{21} cm^{-3}$ for the plugs. An anneal at 900°C was used to activate and provide inert ambient for diode passivation to be performed. Finally, a 1.6um thick PE-TEOS (plasma enhanced tetraethyl orthosilicate) oxide was deposited and chemical mechanical polished back to 0.9um prior to via contact. Low resistance contacts were made by contact titanium sputter, silicidation, and tungsten fill. Finally, a chemical mechanical polish (CMP) was performed followed by a titanium/titanium-nitride/aluminum-copper/titanium-nitride stack for interconnect and contact pads.

The switch operation was demonstrated on a 10-Gb/s 2^{31}-1 non-return-to-zero (NRZ) Pseudo Random Bit Stream (PRBS) driving a lithium niobate Mach-Zehnder modulator. The source was a tunable laser set to 1533nm. The data rate was limited by available test equipment. The switch was activated with a 0.57V supplied square-wave through a ground-signal-ground (GSG) microwave probe. The probe was not terminated. Since the switch impedance is substantially larger than 50Ω, reflection at the device nearly doubles the applied voltage. The switch state is switched every 6.4ns in square wave fashion and the Thru port response is depicted in Fig. 3a and 3b. An extinction of 16dB was measured in the Thru port and the switch 10-to-90 percent switch time was measured to be 2.4ns. An eye-diagram of the transmitted data in the Thru port is shown in Fig. 3c. The synchronous measured
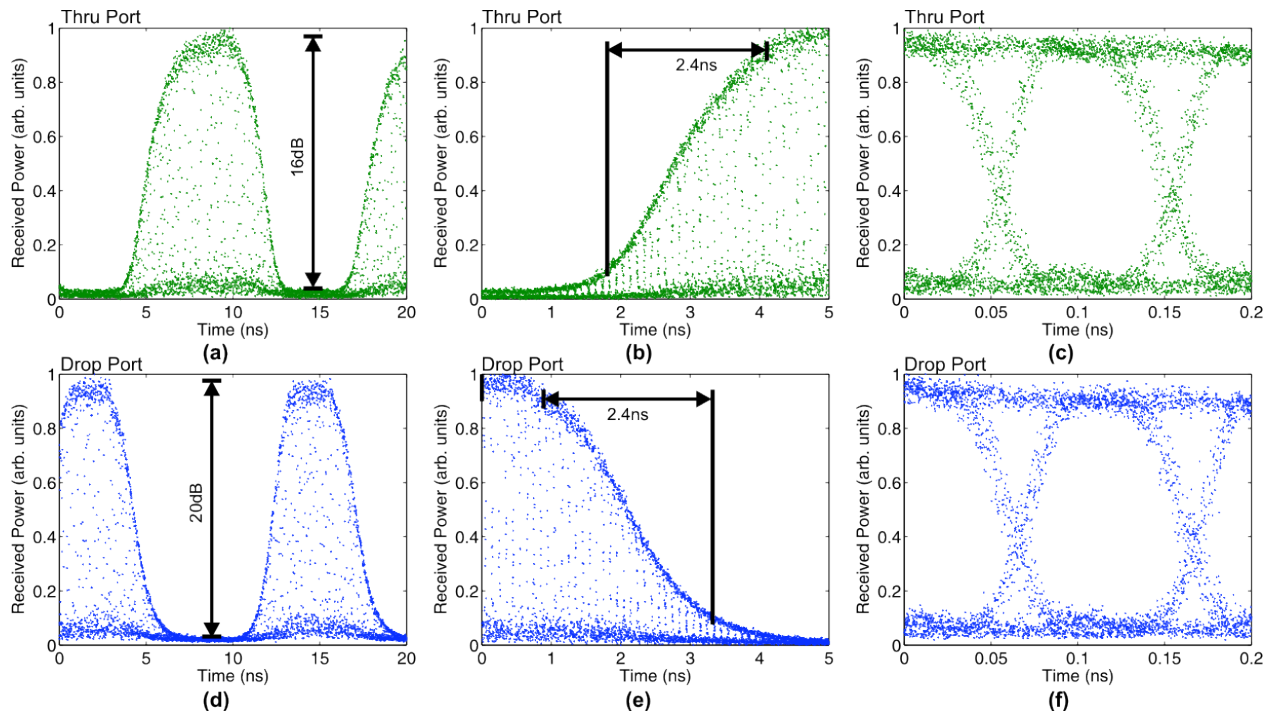
Figure 3. (a) Thru port output versus time switching a 10Gb/s data stream every 6.4ns demonstrating an extinction of -16dB. (b) A close-up of the switch transition in the Thru port indicating a 10-to-90% rise time of 2.4ns. (c) Eye-diagram of the 10Gb/s data stream transmitted at the output of the Thru port of the switch. (d) Synchronous Drop port output versus time with 10Gb/s data stream switched every 6.4ns demonstrating an extinction -20dB. (e) A close-up of the switch transition in the Drop port indicating a 90-to-10% fall time of 2.4ns. (f) Eye-diagram of the 10Gb/s data stream transmitted at the output of the Drop port of the switch.

switch response in the Drop port is shown in Fig. 3d and 3e. An extinction of 20dB was measured in the Drop port and along with a 10-to-90 percent switch response of 2.4ns. An eye diagram of the 10-Gb/s data stream transmitted through the switch to the Drop port is shown in Fig. 3f. The open eye diagrams demonstrate that data integrity is maintained through both states and ports of the switch.

In supercomputer networks, the physical latency between nodes is often many nanoseconds and the latencies introduced by communication protocols are much greater. The 2.4ns switching speed offered by this channel selective switch corresponds to the physical latency induced by only ½ meter of optical fiber. While intrachip networks may require higher speed switches, 2.4ns is sufficient for applications with short lengths of fiber between nodes. Still, achieving higher speeds is possible and can be achieved with even smaller active microring and microdisk resonators, or alternatively, with more careful design of the dopant distributions within the structure. Further, reverse-biased operation offers innately higher speeds on account of reduced resistance and capacitance. In the present structure, the reverse-biased mode is almost an order of magnitude faster (τ=120ps) than the forward-biased approach. The challenge is in achieving a sufficiently large reverse-bias induced frequency shift. However, we have demonstrated a reverse-biased modulator with acceptable modulation depth. Future efforts will be concentrate on improving device speed and modulation depth.

3. Conclusions

The first high-speed, 2nd-order, silicon microdisk channel selective switch has been demonstrated. The switch achieves a switching speed of 2.4ns with a flat-top ~40GHz filter bandpass and 20dB extinction in the Thru port. The realized extinction in switching 10Gb/s data stream is 16dB in the Thru port and 20dB in the Drop port. The switch is constructed of the smallest active microdisk resonators demonstrated to date with a radius of R=3um. The small size enables a massive 4.2THz (32nm) FSR that covers the C-band and could enable upto 40+ channels with a 100-GHz channel separation to be integrated onto a single 4-port switch. This small, high-speed, low-power switch forms the building block for richly interconnected short-range optical networks such as the three-dimensional mesh networks connecting high-performance supercomputers. Further, high-speed (τ=120ps) reverse-biased modulators, also with 4.2THz FSRs have been demonstrated. To our knowledge, these are the largest FSRs demonstrated in resonant modulators and switches.

4. References

1. William M. Green, Michael J. Rooks, Lidija Sekaric, and Yurii A. Vlasov, *Optics Express*, **15**, p. 17106 (2007)

2. A. Liu, R. Jones, L. Liao, D. Samara-Rubio, D. Rubin, O. Cohen, R. Nicolaescu, and M. Paniccia, "A high-speed silicon optical modulator based on a metal-oxide-semiconductor capacitor," *Nature* **427**, 615-618 (2004)

3. Q. Xu, B. Schmidt, S. Pradhan and M. Lipson, "Micrometre-scale silicon electro-optic modulator," *Nature* **435**, 325-327 (2005)

4. C. Gunn, Paper 6125-1, Photonics West, San Jose, January 2006, *Proceedings of SPIE* Vol. #6125

5. R. A. Soref, and B. R. Bennett, "Electrooptical Effects in Silicon," *IEEE J. Quantum Electronics*, **QE-23**, pp. 123-129 (1987)